Comments on Inorganic Chemistry
Publication details, including instructions for authors and subscription information:
http://www.informaworld.com/smpp/title~content=t713455155

STRUCTURAL MAPPING OF HYBRID METAL PHOSPHONATE CORROSION INHIBITING THIN FILMS

Maria Papadaki[a]; Konstantinos D. Demadis[a]
[a] University of Crete, Heraklion, Crete, Greece

To cite this Article Papadaki, Maria and Demadis, Konstantinos D.(2009) 'STRUCTURAL MAPPING OF HYBRID METAL PHOSPHONATE CORROSION INHIBITING THIN FILMS', Comments on Inorganic Chemistry, 30: 3, 89 — 118
To link to this Article: DOI: 10.1080/02603590903320916
URL: http://dx.doi.org/10.1080/02603590903320916

Comments on Inorganic Chemistry, 30: 89–118, 2009

ISSN: 0260-3594 print
DOI: 10.1080/02603590903320916

Taylor & Francis
Taylor & Francis Group

STRUCTURAL MAPPING OF HYBRID METAL PHOSPHONATE CORROSION INHIBITING THIN FILMS

MARIA PAPADAKI and KONSTANTINOS D. DEMADIS

University of Crete, Heraklion, Crete, Greece

The constant growth in the area of metal phosphonate materials is exemplified with rich chemistry and a variety of applications. From the multitude of subjects related to metal phosphonates, we have decided to focus on metal phosphonate coordination polymers as corrosion inhibitors in the present Comment. A plethora of metal phosphonate organic-inorganic polymeric hybrid materials have been synthesized, structurally characterized, and evaluated for their anticorrosion properties for the protection of carbon steels. These materials are composed of a metal ion (usually Zn^{2+}, Ca^{2+}, Sr^{2+}, Ba^{2+}, etc.) and polyphosphonate ligands such as AMP (amino-*tris*-(methylenephosphonate) and HDTMP (hexamethylenediamine-*tetrakis*(methylenephosphonate), or carboxyphosphonate ligands, such as PBTC (2-phosphonobutane-1,2,4-tricarboxylate) and HPAA (hydroxyphosphonoacetate). Their corrosion inhibition performance has been evaluated and some interesting conclusions are drawn relating molecular structure to inhibitory activity.

***Keywords*: frameworks, hybrids, inhibition, metal phosphonates corrosion, MOF**

Address correspondence to Konstantinos D. Demadis, Crystal Engineering, Growth and Design Laboratory, Department of Chemistry, University of Crete, Voutes Campus, Heraklion, Crete, GR-71003, Greece. E-mail: demadis@chemistry.uoc.gr

1. INTRODUCTION

The definition of metallic corrosion varies according to the particular discipline of science considered. All definitions, albeit diverse, have a significant common theme: the change of the mechanical properties of metals in an undesirable way. More specifically, ISO 8044 defines corrosion as a "physico-chemical interaction, that is usually of an electrochemical nature, between a metal and its environment which results in changes in the properties of the metal and which may often lead to impairment of the function of the metal, the environment, or the technical system of which these form a part".[1] Technology notwithstanding, the "economics" of corrosion is a key factor in the marketplace. Its cost has been estimated (based on several reports) to be in the order of an astonishing 1–5% of national GDP.[2] World-wide cost of corrosion for the production of all grades of pulp is about $3 billion/year. These numbers do not include the cost of lost production, shutdowns to make repairs to corroded equipment, etc. Corrosion cost in the US electric power industry reaches $10 billion/year, according to the Electric Power Research Institute (EPRI).[3] Also, it has been reported by EPRI that corrosion is the cause for more than 55% of all unplanned outages and it adds over 10% to the average annual household electricity bill. The impact of corrosion on all branches of industry in almost all countries can be observed. For example, in 1993 it was estimated that 60% of all maintenance costs for North Sea oil production platforms were related to corrosion either directly or indirectly. A report on inspection results of several offshore production plants showed that corrosion was a factor in 35% of structures, 33% of process systems and 25% of pipelines. The importance of preventing corrosion issues is also exemplified in the recent unfortunate incident of 267,000 gallons of crude oil spillage in Prudhoe Bay, Alaska. BP was accused of faulty maintenance of a corrosion-laden pipeline.[4]

Corrosion management can be achieved in several ways, one of which is based on chemical means. Chemical additives are introduced to the process stream in contact with the metallic surface to be protected. These are called corrosion inhibitors. They are chemical additives that delay or (ideally) stop metallic corrosion.[5]

There exists a diverse list of corrosion inhibitors that are effective for the decrease of metallic corrosion in a wide range of pH conditions. However, within the framework of the present review we will limit our

discussion to the class of inhibitors that operate by complexation with metal cations. Kuznetsov has named these "corrosion inhibitors of the complexing type."[6] There is a surprising wealth of "nuggets" of inorganic and coordination chemistry, as well as chemistry of metal-organic

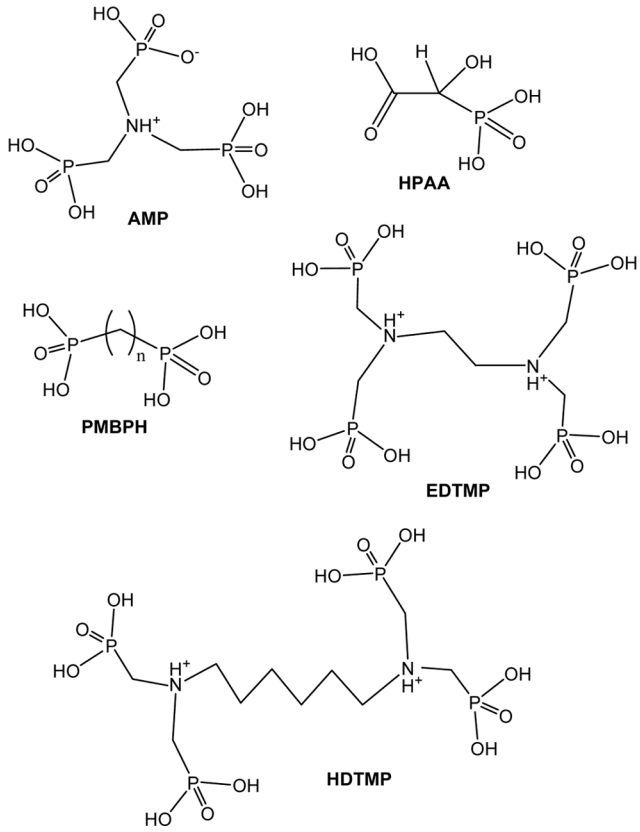

Figure 1. Some representative schematic structures of phosphonate-containing ligands that have been used as corrosion inhibitors. Abbreviations: AMP = amino-tris(methylenephosphonic acid), HPAA = hydroxyphosphonoacetic acid, PMBPH = polymethylenebisphosphonic acid, EDTMP = ethylenediamine-tetrakis(methylenephosphonic acid), HDTMP = hexamethylenediamine-tetrakis(methylenephosphonic acid), PBTC = 2-phosphonobutane-1,3,4-tricarboxylic acid, HEDP = hydroxyethyledene-bisphosphonic acid, AEPA = aminoethylphosphonic acid, OCPA = octylphosphonic acid, AATP = 3-anisalidene-amino-1,2,4-triazole phosphonate, HOC_3NP_2 = N,N-tetramethyl-bis(phosphonate)-3-hydroxylpropyl-bis(methylene)amine.

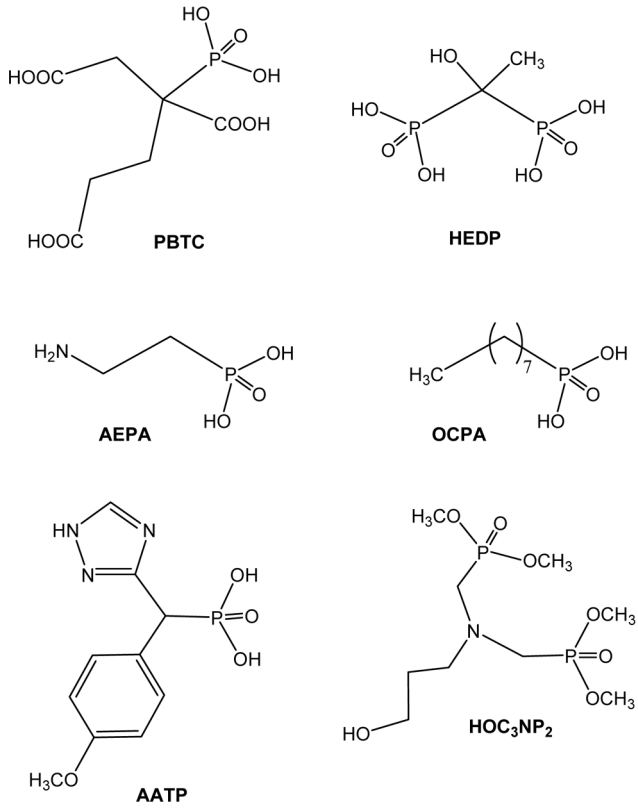

Figure 1. Continued.

hybrids. In our discussion (and within the scope of this journal) we will consider a particular type of corrosion inhibitors, namely (poly)-phosphonic acids.

At appropriate pH regions (depending on the particular application) phosphonic acids exist in their (partially or completely) deprotonated form. There are several reports on the deprotonation chemistry of phosphonic acids.[7] Thus, in the presence of metal cations (commonly alkaline earth metals), they form sparingly soluble compounds, which eventually precipitate onto the metallic surface to form an ideally two-dimensional protective thin film. Such phosphonate inhibitors for diverse water-related technologies constitute a long list; some representative examples are shown in Figure 1.

Widely used examples of organic phosphonic acids in commercial applications are 1-hydroxyethane-1,1-diphosphonic acid (HEDP), amino-*tris*(methylenephosphonic acid) (AMP), hydroxyphosphonoacetic acid (HPAA), and 2-phosphonobutane-1,2,4-tricarboxylic acid (PBTC). Phosphonates are introduced into the system to be protected in the acid form or as alkali metal water-soluble salts, but readily form more stable complexes with other metal cations found in the process stream (most commonly Ca, Mg, Sr or Ba), depending on the particular application. Research in this area has been stimulated by the need to develop inhibitor formulations that are free of chromates, nitrates, nitrites, inorganic phosphorus compounds, etc. Phosphonates, when blended with certain metal cations and polymers, reduce the optimal inhibitor concentration needed for inhibition due to synergistic effects. Synergism is one of the important effects in the inhibition process and serves as the basis for the development of all modern corrosion inhibitor formulations.

In spite of the significant body of literature, studies on the molecular identity of the thin protective metal-phosphonate films lag behind. In this paper we review the utility of metal phosphonate materials as corrosion inhibitors, keeping the focus on their structural aspects. We also discuss the potential link between structure and anticorrosion performance by presenting and analyzing relevant data from literature and our own efforts.

2. CURRENT LITERATURE ON CORROSION PROTECTION BY PHOSPHONATES

In this section we briefly review the state-of-the-art of the field of phosphonates as corrosion inhibitors. We have categorized this section according to the metal surface that is protected by phosphonates/metal phosphonates, with a subsection dedicated to the use of phosphonates in anti-corrosive paints.

2.1. Steel

Mixtures of 2-aminothiophenol (ATP) and 1-hydroxyethylidene-bis(phosphonic acid) (HEDP) show a cooperative effect of inhibition of stainless steel (SS 41).[8] The actual role of HEDP was explained in terms of its scale inhibition activity towards $FeCO_3$.

Kuznetsov et al. have studied the inhibitor efficiency of various phosphonate inhibitors of the aminomethylenephosphonate type ($R–N–CH_2–PO_3H_2$).[9] The protective properties of aminophosphonic acids and their magnesium and calcium complexes were studied in soft water. 1,1-hydroxycarboxypropane-3-amino-di(methylenephosphonic) and hexamethylenediamine-N,N-tetra(methylene-phosphonic) acids could suppress the corrosion of steel in water completely. Kouznetsov proposed that metal phosphonate complexes are much more effective than the corresponding acids; if the complexing agent is fixed, then the stability constants of the complexes become the major factor. For phosphonates of Mg^{2+} and Ca^{2+}, which are usually less stable than the corresponding iron complexes, the dependence of the protective concentration on stability constant passes through a maximum; the complexes of those acids whose own protective properties are weaker are more effective. Imino-N,N-diacetic-N-methylenephosphonic acid can serve as an example. By contrast, the relatively more stable complexes, for example calcium nitrilotri(methylenephosphonate) (AMP), are much less effective than the acid itself.

Molybdate is a well-known corrosion inhibitor. Its combination with phosphonates enhances corrosion efficiency.[10] A level of 300 ppm MoO_4^{2-} had only 32% efficiency in inhibiting the corrosion of mild steel immersed in a neutral aqueous environment containing 60 ppm Cl^-, whereas a formulation of AMP (50 ppm) – MoO_4^{2-} (300 ppm) – Zn^{2+} (50 ppm) exhibited 96% inhibition efficiency. The lower inhibition efficiency in the former case was due to the dissolution of the protective film formed on the metal surface, and getting precipitated in the bulk of the solution; this system controlled the anodic reaction only. The latter system controlled both the anodic and cathodic reactions; the dissolution of the protective film formed on the metal surface was reduced to a greater extent.

Protective layer formation of α,ω-diphosphono-alkane compounds on iron surface was studied.[13] Layer formation proved to be a spontaneous process on iron, and can be accomplished by simple immersion into an aqueous solution of phosphonate additives, resulting in a thin dense multimolecular adsorption layer with a high corrosion protection effect. It was concluded that the mechanism of inhibition was anodic type, hindering active iron dissolution due to the blocking of the metal surface. The protective layer formation is complete after a few days of immersion, resulting in a thin but dense multimolecular adsorption layer.

"Self-healing" effect of diphosphonates was demonstrated. Based on the high corrosion protection effect, surface modification by diphosphonates may be regarded as potential anticorrosive treatment.

Surface treatments have been carried out on carbon steel in solutions containing different phosphonates.[14] The compounds were dissolved in an ethanol/water mixture (80:20). Corrosion protection afforded by laurylphosphonic acid (LPA), ethyllaurylphosphonate (ELP; also called lauryl phosphonic acid monoethylester) and diethyllaurylphosphonate (DELP) was studied by steady-state current-voltage curves and electrochemical impedance measurements with a rotating disc electrode. Corrosion protection was only obtained for the ethyllaurylphosphonate (ELP), which was able to form a relatively thick film on the carbon steel surface. Electron probe microanalysis corroborated that the film is thick and porous. Infra-red spectroscopy indicated that the film was formed by reaction of the organic phosphonate with the steel surface to produce a metal salt.

The effect of phosphonates used in Russian heat-power engineering on the corrosion of carbon steel in deaerated delivery water at 90°C was studied.[15] It was demonstrated that introduction of phosphonates reduced the susceptibility of steel to local corrosion. A Zn^{2+} complex of hydroxyethylidenediphosphonic acid (OEDP–zinc) was the most effective inhibitor of the anodic reaction.

For the protection of carbon steel from corrosion, aminotrimethylidenephosphonic acid (AMP) was more effective than 1-hydroxyethylidene diphosphonic acid (HEDP), N,N-dimethylidenephosphonoglycine (DMPG), 1-ethylphosphonoethylidenediphosphonic acid (EEDP), and ethylenediaminetetramethylidenephosphonic acid (EDTMP).[16] A 20-min treatment in 1.0 M of AMP at pH 0.23 at 45°C formed an anti-corrosive complex film that was composed of 48.4% O, 28.6% P, 7.0% Fe, 4.3% N, and 11.7% C, based on XPS and Auger electron spectroscopy. From differences in binding energies of Fe, N, and O, in the shift of C–N and P–O vibration, in the reflection FT-IR spectra, and in the change of P–OH and Fe–N vibration before and after film formation, it was deduced that N and phosphonate O in AMP were coordinated with Fe^{2+} in the film.

The corrosion inhibition of iron in 0.5 M sulfuric acid by N, N-dipropynoxy methyl amine trimethyl phosphonate was investigated by means of potentiodynamic polarization and electrochemical impedance spectroscopy (E.I.S.) techniques.[17] N,N-dipropynoxy methyl

amine trimethyl phosphonate was studied in concentrations from 40 ppm to 320 ppm at a temperature of 298 K. The results revealed that the inhibition mechanism of N,N-dipropynoxy methyl amine trimethyl phosphonate is a combination of anodic and cathodic type. It is also found that this inhibitor obeys the Frumkin adsorption isotherm and Flory-Huggins isotherm based on a substitutional adsorption process.

The role of pH and Ca^{2+} in the adsorption of an alkyl N-aminodimethylphosphonate on mild steel (E24) surfaces was investigated by XPS.[18] Fe 2p3/2 and O 1 s spectra showed that the oxide/hydroxide layer developed on the steel surface, immersed in the diphosphonate solution ($7 < pH < 13$, without Ca^{2+}) or in a filtered cement solution (pH 13, 15.38 M of Ca^{2+}), consists of Fe_2O_3, covered by a very thin layer of FeOOH (goethite). The total thickness of the oxide/hydroxide layer was $\sim$3 nm and was independent of the pH and the presence/absence of Ca^{2+}. In the absence of Ca^{2+} ions, the N 1 s and P 2p spectra revealed that the adsorption of the diphosphonate on the outer layer of FeOOH took place only for pH lower than the zero charge pH of goethite (7.55). At pH 7, the adsorbed diphosphonate layer was continuous and its equivalent thickness was $\sim$24 Å (monolayer). In the presence of Ca^{2+} ions, the C 1 s and Ca 2p signals indicated that Ca^{2+} was present on the steel surface as calcium phosphonate (and $Ca(OH)_2$, in very small amounts). The adsorption of the diphosphonate molecules on the steel surface was promoted in alkaline solution ($pH > 7.55$) by the divalent Ca^{2+} ions that bridged the O^{2-} of goethite and the $P–O^-$ groups of the diphosphonate molecules. The measured values for the Ca/P intensity ratio were in the range 0.75–1, which suggested that the diphosphonate molecules were adsorbed on steel forming a coordination polymer cross-linked by Ca^{2+} through their phosphonate groups. In the presence of Ca^{2+} ions in alkaline solution, the adsorbed diphosphonate layer was discontinuous and the surface coverage was found $\sim$34%.

The effect of a new class of corrosion inhibitors, namely piperidin-1-yl-phosphonic acid (PPA) and (4-phosphono-piperazin-1-yl)phosphonic acid (PPPA) on the corrosion of iron in NaCl medium, was investigated by electrochemical measurements.[19] Potentiodynamic polarization studies clearly revealed the type of the inhibitor. The addition of increasing concentrations of phosphonic acids caused a shift of the pitting potential (E_{pit}) in the positive direction, indicating the inhibitive effect of the added phosphonic acid on the pitting attack. The potential of corrosion was moved towards negative values and the corrosion current was

reduced. The values of the current were lower in the presence of PPA and PPPA. This was explained by the fact that most of the surface of the electrode was covered by the molecules adsorbed. PPPA had a strongly inhibitive effect on chloride pitting corrosion. It was proposed that the addition of the $NCH_2PO_3H^-$ group (center adsorption) in the PPA para-position, giving PPPA, reinforced the active sites of this molecule and consequently increased its inhibition efficiency.

Phosphonate layer formation on a passive iron surface was investigated by electrochemical and atomic force microscopy techniques.[23] It was found that phosphonate groups bond more strongly to the oxide surface, while metallic iron surface is disadvantageous for phosphonate layer formation in aqueous solutions. The rate of anodic dissolution was continually decreasing due to the time-dependent formation of protective phosphonate layer. The kinetics of phosphonate layer formation on passive iron was determined by the potential applied for preceding passive film formation. The size and shape of iron oxide grains depended slightly on the potential of passivation. Changes in morphology due to the phosphonate layer formation were recorded by AFM.

The passivating ability of the zinc complex of the 1-hydroxyethane-1,1-diphosphonic acid (HEDP) in a borate buffer solution was studied.[25] An *in situ* ellipsometric method was used to study the mechanism of formation of a protective film on iron in the presence of HEDP, Zn-HEDP, and $ZnSO_4$ in the course of the cathodic polarization of the electrode. The studies of Zn-HEDP adsorption on iron (at $E = -0.65$ V) in combination with X-ray photoelectron spectroscopy (XPS) showed that on the metal surface a multilayer protective film formed consisting of an internal layer of $Zn(OH)_2$ and an outer layer consisting of HEDP complexes with Fe^{2+} and/or Zn^{2+}. It was found that the thickness of the passivating film does not exceed 60 Å, of which 7–10 Å correspond to the sparingly soluble $Zn(OH)_2$.

Electrochemical techniques were used for investigating the inhibitory activity on carbon steel of thiomorpholin-4-ylmethyl-phosphonic acid (TMPA) and morpholin-4-methyl-phosphonic acid (MPA) in natural seawater.[27] Measurement of the free corrosion potential indicated that the phosphonic acids tested inhibit the corrosion of carbon steel in seawater. Potentiodynamic polarization curves showed clearly proved that addition of these molecules is responsible for corrosion current density decrease and a corresponding reduction of the corrosion rate. The phosphonic acids tested as corrosion inhibitors of carbon steel in natural

seawater are effective even at low concentrations. FT-IR spectroscopy was used to obtain information on the interaction between the metallic surface and the inhibitors. The morphology of the metal surface in the uninhibited and inhibited solution was examined using SEM/EDS.

2.2. Copper

New corrosion inhibitors, namely 3-vanilidene-amino-1,2,4-triazole phosphonate (VATP) and 3-anisalidene amino 1,2,4-triazole phosphonate (AATP), were synthesized and their action along with biocide on corrosion control of copper in neutral aqueous environment has been studied.[12] Potentiodynamic polarization measurements and electrochemical impedance spectroscopy (EIS) had been employed to analyze their inhibition behavior. VATP showed better protection over the other inhibitors used. The dissolution of copper in presence of VATP and AATP with biocide mixture is negligible compared to blank. A combination of electrochemical methods and surface examination techniques are used to investigate the protective film and explain the mechanistic aspects of corrosion inhibition.

A thin-film coating consisting of Zr^{4+} and octadecyl phosphonate provided inhibition of O_2 reduction for Cu-rich aluminum alloys, such as AA2024-T3.[24] The coating procedure produced films with thicknesses approaching that of a self-assembled monolayer. Using constant-potential experiments, the current density for the O_2 reduction reaction was shown to decrease by 2 orders of magnitude following five treatments. Auger electron spectroscopy of the coating showed that both Zr and P are present at the alloy surface following treatment. Characterization of the coating showed it to be hydrophobic, with the octadecyl chains being in a liquid-like environment.

2.3. Zinc

The reaction of water-based solution of 1,5-diphosphono-pentane (DPP) and 1,7-diphosphonoheptane (DPH) with high purity polycrystalline zinc surface was investigated at room temperature.[22] XRD and XPS studies confirmed the formation of a crystalline zinc–phosphonate film on the metal surface. The assembled layers gave hydrophilic properties to the surface. A conversion-type interaction of diphosphonic acid compounds with the oxidized zinc surface was unambiguously shown by XPS

analysis. Conclusive results were obtained by synthesized zinc–diphosphonate model compounds modeling the ones deposited on the zinc surface, revealing a ~1:1 molar ratio of the phosphonate groups with zinc. Reactions with both diphosphonates resulted in significant protective effect of zinc against corrosion, although the structure and quality of the formed layers exhibited marked differences. The in-depth distribution of the composition and dissimilarity of the layer thickness were determined by glow discharge optical emission spectrometry (GD-OES). The corrosion inhibition was explained by the formation of insoluble zinc–phosphonate salt on the zinc surface, blocking the zinc dissolution process.

Efforts to understand the inhibition mechanism of 1,5-diphosphonic acid on mechanically polished zinc substrates were focused on the surface structure of layers formed in aqueous and ethanol solutions.[28] In spite of the differences noted in the protective layers formed in ethanol and in aqueous solution, their protection efficiency was identical after ~4 h testing. Based on EIS, XPS and GD-OES data, a simple oxide–hydroxide/diphosphonate model of the interface was proposed. Both XPS and GD-OES showed unambiguously that the surface film contained large amounts of Zn, comparable to the P content, especially when the layer deposition originated from an aqueous solution of 1,5-diphosphonic acid. On that basis, it was concluded that the surface film consisted of a zinc–phosphonate layer.

2.4. Aluminum

The cooperative effect of Ca^{2+} and tartarate ion on the corrosion inhibition of pure aluminum in an alkaline solution was investigated by hydrogen collection, electrochemical methods and XPS.[11] The results of electrochemical experiments showed that the inhibition by Ca^{2+} was enhanced by the addition of tartarate ion, while tartarate ion itself has only a little inhibition effect. Analysis by XPS showed that Ca^{2+} and tartarate ions did not contribute to the formation of the surface film on aluminum. This fact indicates that these two ions act as interface inhibitor. The cooperative effect of the two ions might be due to formation of a complex, which makes it easier for Ca^{2+} to adsorb on the aluminum surface.

The amino-tris-(methylenephosphonic acid) (AMP) layers were adsorbed on the surface of AA6061 aluminum alloy for improving the

lacquer adhesion and corrosion inhibition as a substitute for chromate coatings.[21] The surface structure and features of the AMP layers on AA6061 aluminum alloy were investigated by means of XPS and ATR-FTIR analysis. The analyzed results showed that the AMP adsorption layers adsorbed on the surface of aluminium alloy *via* acid-base interaction in a bi-dentate conformation. After the AMP layers were coated with epoxy resin, the layers showed good adhesive strength and favorable corrosion resistance in contrast to chromate coatings.

2.5. Phosphonates in Anti-Corrosive Paints

Two novel phosphonated methacrylate monomers were successfully synthesized and subsequently incorportated into adhesion/anticorrosive coatings.[20] Specifically, they were propyl N,N-tetramethyl-bis(phosphonate)-2-hydroxyl-bis(methylene)amine methylmethacrylate (MAC_3NP_2) and 2-[2,2-bis(diisopropoxyphosphoryl)ethoxy]-methylmethacrylate, (MAC_3P_2). The phosphonic forms of each monomer were blended with ~85% w/w acrylates (tripropyleneglycol-diacrylate and hexanediol-diacrylate) and ~6% w/w of the photo sensitive initiator DarocurVVR. Along with a monophosphonic monomer synthesized in a previously (MAC3P), they were polymerized on Q-panels under ultraviolet light, and then subjected to the salt spray test (~0.5 M NaCl at 35°C) for a duration of up to 50 days. The results indicated that acrylate blends with low concentration of the bisphosphonic compound MAC3P2 had excellent resistance to corrosion, thus excellent adhesive properties. Importantly, these coatings were formed without the use of a hydrophobic polymer matrix or solvents.

The efficiency of calcium tripolyphosphate and zinc tripolyphosphate as anticorrosive pigments for paints in aggressive environments was studied.[26] Alkyd and epoxy paints, of the solvent borne type, containing 30% by volume (v/v) of the pigment, were formulated. The pigment volume concentration/critical pigment volume concentration (PVC/CPVC) ratio was fixed at 0.8. In a second stage, water-borne paints containing 30% v/v of both tripolyphosphates and different PVC values (20 and 25%) were also formulated. Finally, standardized accelerated (salt spray and humidity chamber exposure) and electrochemical impedance spectroscopy (EIS) tests were used to assess the protective performance of the coatings. Analysis and interpretation of the experimental data showed that both, calcium and zinc tripolyphosphates

inhibited corrosion of painted steel panels exposed to aggressive environments.

3. STRUCTURAL FEATURES OF CORROSION-INHIBITING METAL PHOSPHONATE FRAMEWORKS

Although there is a plethora of publications on the anticorrosion effects of phosphonates and/or metal phosphonates on various metallurgies, there are very limited published data on the identity of the protective film at the molecular level. In this section we will present several examples, mostly originating from our research group, on the subject. The focus will be on the structural features of metal phosphonate frameworks that have exhibited anticorrosion performance. However, we are referring the reader to several reviews that analyze in detail the scope of structural chemistry of metal phosphonate materials.[29–35]

In the structure of Zn-AMP (Figure 2),[36] AMP maintains its "zwitter ionic" character[37] in the crystal lattice because each phosphonate group is singly deprotonated, whereas the N atom is protonated. The Zn^{2+} cation is coordinated by three phosphonate oxygens and three H_2O molecules. AMP forms an eight-membered chelate ring with the Zn^{2+} cation. The bond angles indicate a slightly distorted octahedral geometry, with the largest deviation being 166.90(6)°. The third phosphonate arm, surprisingly, is not coordinated to the Zn^{2+} cation, but is exclusively involved in hydrogen bonding.

A zigzag chain is formed by the Zn^{2+} cation and the coordinating portion of AMP. The Zn^{2+} centers are located at the corners of the zigzag chain, whereas the "linear" portion of the zigzag is made of the non-coordinated, hydrogen-bonded phosphonate groups. The presence of a non-coordinated, singly deprotonated phosphonate group in the

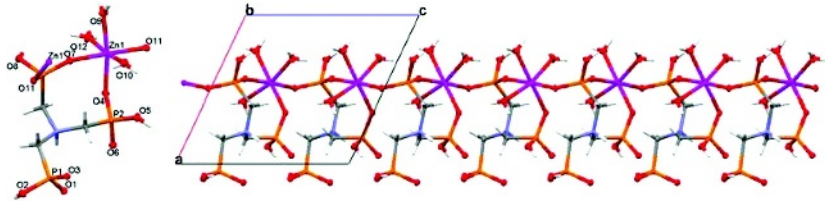

Figure 2. Structure of the coordination polymer $Zn(AMP)(H_2O)_3$: the asymmetric unit (left) and the structure of the layer (right). The uncoordinated phosphonate group is located at the bottom of the layer, facing down.

lattice is somewhat surprising. This phosphonate moiety participates in a complicated hydrogen bonding network that presumably "relieves" the presence of the negative charge.

Clearfield et al. have reported a similar zinc-AMP material having the formula $Zn_2[HO_3PCH_2NH(CH_2PO_3)_2]$, which features a 3D network built from ZnO_4 tetrahedra linked together by bridging phosphonate groups.[38] The two zinc ions in the asymmetric unit are tetrahedrally coordinated by four phosphonate oxygen atoms of four ligands. Each ligand connects with eight zinc atoms.

The crystal structure of Zn-HDTMP (Figure 3) shows that it is a three-dimensional (3D) coordination polymer.[39] The Zn-O distances are unexceptional and consistent with other structurally characterized zinc-phosphonates.[40–45] The Zn^{2+} cation is found in a distorted octahedral environment that is formed exclusively by phosphonate oxygens.

The C_6 carbon chain does not possess the expected zigzag configuration; however, the portion C(2)-C(3)-C(5)-C(6) is in a "syn" rather than "anti" configuration.

The crystal structure of Ca-PBTC (Figure 4) reveals a polymeric material with PBTC acting as a tetradentate chelate.[46] The Ca^{2+} center is seven-coordinated in a capped octahedral environment, bound by two phosphonate oxygens, three carboxylate oxygens and two water molecules. The phosphonate oxygens act as bridges between two neighboring Ca centers, located 6.781 Å apart. All three carboxylate oxygens are protonated. The protonated –COOH group is coordinated to the Ca through the carbonyl atom. This is consistent with the long Ca–O(=C) distances

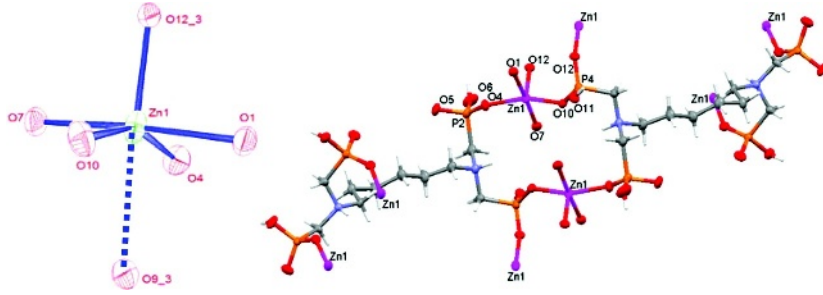

Figure 3. Structure of the coordination polymer Zn(HDTMP)(H_2O): the Zn^{2+} coordination environment (left) and portion of the structure showing the extensive 18-membered ring (right).

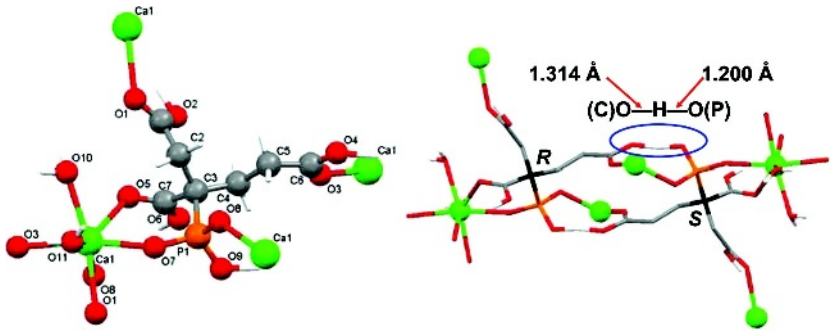

Figure 4. Structure of the coordination polymer $Ca(PBTC)(H_2O)_2 \cdot 2\,H_2O$: the coordination ability of $PBTC^{2-}$ binding neighboring Ca^{2+} ions (left) and portion of the structure showing the R and S isomers, as well as stabilization by hydrogen bonding (right).

of 2.470(2) and 2.448(2) A. Such Ca–O=C(OH) coordination modes are rare.[47,48] The bridging $-PO_3^{2-}$ tetrahedral and the CaO_7 polyhedra are arranged in a zigzag chain configuration. Both *R* and *S* stereoisomers (according Cahn-Ingold-Prelog sequence) of PBTC are present in the structure of $Ca(PBTC)(H_2O)_2 \cdot 2\,H_2O$ in a regular pattern.

In the 3D structure of Sr(Ba)-HPAA (Figure 5), each HPAA links to five symmetry-equivalent, 9-coordinated Sr(Ba) centers through the phosphonate group (bridging three Sr(Ba) ions), the carboxylate group

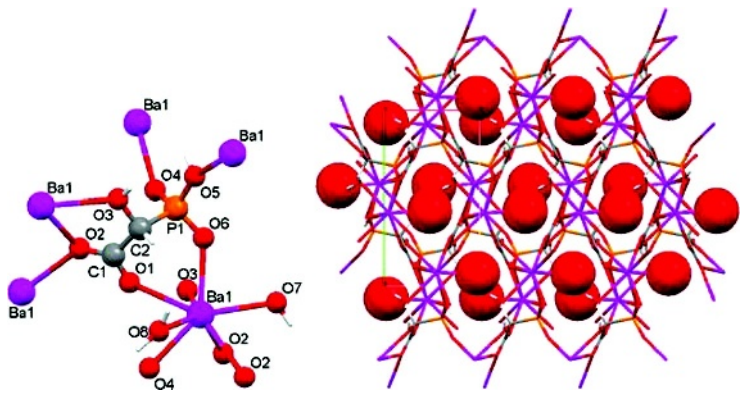

Figure 5. Structure of the isostructural coordination polymers Ba(or Sr)$(HPAA)(H_2O)_2$: the coordination ability of $HPAA^{2-}$ binding neighboring Ba^{2+} ions (left) and portion of the 3D structure showing the Ba-bound waters as red spheres (right).

(bridging three Sr(Ba)) and the protonated hydroxyl moiety (coordinating terminally one Sr(Ba) center).[49,50]

There are no H_2O's of crystallization, but two Sr(Ba)-coordinated waters. In structures the *R* and *S* HPAA isomers are interwoven into a complicated 3D arrangement.

Slight changes in pH afford a new phase, $Sr(HPAA)(H_2O)_3 \cdot H_2O$. Structural features are presented in Figure 6. This is a 2D, layered coordination polymer consisting of "$Sr(HPAA)(H_2O)_3$" units that are connected through a Sr–O(carboxylate) linker. The Sr atoms are 8-coordinated. Sr–O bond distances range from 2.5030(17) to 2.6916(18) Å. Consequently, each $HPAA^{2-}$ ligand is coordinated to three symmetry-related Sr^{2+} centers. On the basis of the virtually equal C–O bond lengths (C(2)–O(5) 1.258(3) Å and C(2)–O(6) 1.260(3) Å) the negative charge is delocalized over the entire O−C−O moiety.

The isostructural Sr(Ba)-HDTMP compounds form a zigzag, corrugated arrangement (see Figure 7) with an "opening" angle of (P)O−M−O(P) of 115.59(9) (for Sr) and 117.66(8) (for Ba).[51] The coordination environment of the eight-coordinated Sr^{2+} (Ba^{2+}) center in both structures can be described as a bicapped octahedron. The M−M−M [M=Sr,Ba] angles are very similar, 150.3(2) for Sr-HDTMP and 149.7(2) for Ba-HDTMP.

The crystal structures of the Ca(Sr)-EDTMP frameworks reveal extended, 1D coordination polymers with EDTMP2- acting as both chelating and bridging ligand (Figure 8).[52] There are some interesting features in these structures that warrant some attention. The $-PO_3H^-$

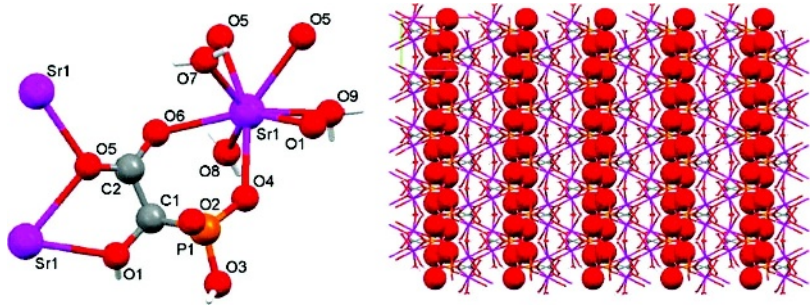

Figure 6. Structure of the coordination polymer $Sr(HPAA)(H_2O)_3 \cdot H_2O$: the coordination ability of $HPAA^{2-}$ binding neighboring Sr^{2+} ions (left) and portion of the 2D layered structure showing the lattice waters between the inorganic layers as red spheres (right).

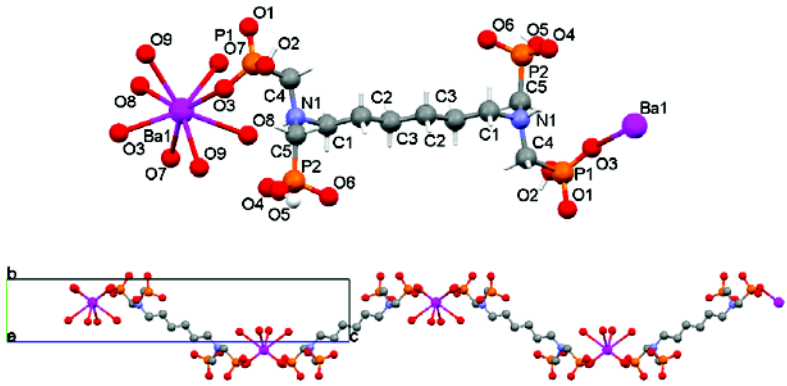

Figure 7. Structure of the isostructural coordination polymers Ba(or Sr)(HDTMP)$(H_2O)_6 \cdot H_2O$: asymmetric unit (left) and portion of the 1D chain structure (right).

group coordinates to Sr^{2+} through only one of its three oxygens. This is in contrast to several literature examples that demonstrate the strong propensity of the $-PO_3H^-$ group to bridge two or more metal centers. Two $-PO_3H^-$ groups, one from each N, form an 11-membered chelate ring with Sr^{2+}. The same function occurs on the other side of the $-CH_2CH_2-$ linker that renders the whole tetraphosphonate a bridge between two Ca^{2+} centers. Thus, one can envision the 1D polymer as a ribbon in a "wave-like" motion composed of Ca-EDTMP-Ca dimers. To the best of our knowledge this coordination mode of EDTMP is

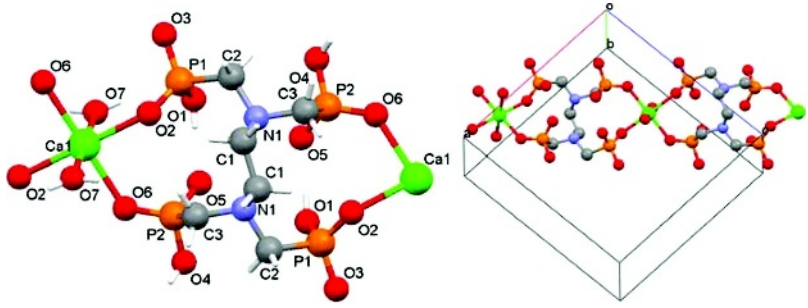

Figure 8. Structure of the isostructural coordination polymers Ca(or Sr)(EDTMP)-$(H_2O)_2 \cdot H_2O$: the Ca-EDTMP-Ca "dimer" (left) and portion of the 1D chain structure (right).

unprecedented. The Sr^{2+} is located in a slightly distorted octahedral environment shaped by four equatorial phosphonate oxygens and two axial H_2O's *trans* to each other. The Sr–O(P) bond distances are 2.4686(18) Å and 2.4884(16) Å, whereas the Sr–O water bond distance is 2.521(2) Å. The water of crystallization rests above a plane formed by four phosphonate oxygens. However, the H_2O molecule forms hydrogen bonds from the "wire" above, with two protonated phosphonic acid moieties ($-P-O_5$–H) and with two phosphoryl oxygens (–P=O_1). The specific bridging mode of EDTMP observed in the structure of Ca(Sr)-EDTMP causes the ligand to acquire a strained position. Thus, the $H_2O-Sr-OH_2$ axial vectors in the dimeric "unit" are not aligned, but form a dihedral angle of 48.49 Å. Very few metal-EDTMP compounds have been reported with metal ions such as Eu^{3+}, Pb^{2+} and Zn^{2+}.[53,54] The coordination mode of EDTMP is distinctly different in these materials.

4. METALLIC CORROSION INHIBITION BY METAL PHOSPHONATE THIN FILMS

Synergistic combinations of 1:1 molar ratio Zn^{2+} and AMP were reported to exhibit superior inhibition performance than either Zn^{2+} or AMP alone.[55–57] However, no mention is made regarding the identity of the inhibitor species involved in corrosion inhibition. Carefully designed corrosion experiments were carried out according to an established protocol[58] in order to verify the literature results and prove that the protective material acting as a corrosion barrier is an organic-inorganic hybrid composed of Zn and AMP. A synergistic combination of Zn^{2+} and AMP in a 1:1 ratio exhibited excellent corrosion protection for carbon steel.[36] Based on mass loss measurements, the corrosion rate for the "control" sample was 2.5 mm/year, whereas for the Zn-AMP protected sample 0.9 mm/year, a 270% reduction in corrosion rate (Figure 9). The filming material is collected and subjected to FT-IR, XRF and EDS studies. These proved unequivocally that the corrosion protection was due to Zn-AMP film formation on the steel surface.

These show that the inhibiting film is a material containing Zn (from added Zn^{2+}) and P (from added AMP) in an approximately 1:3 ratio. Fe was also present, apparently originating from the steel specimen. FT-IR showed multiple bands associated with the phosphonate groups that closely resemble those of an authentically prepared Zn-AMP material.

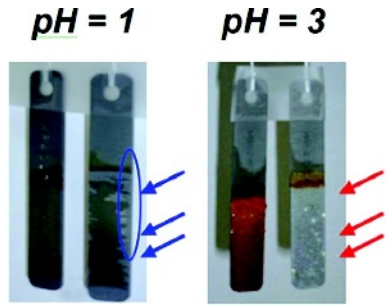

Figure 9. Corrosion protection by Zn-AMP at pH 1 and 3. In both images the "control" is the left specimen and the protected one is the right specimen.

For comparison, EDS and XRF spectra of a "protected" and an "unprotected" region show the presence of Zn and P in the former, but complete absence in the latter. SEM studies gave further information on film morphology (Figure 10).

Another synergistic system that was meticulously studied was that of Zn^{2+} and HDTMP. A synergistic combination of Zn^{2+} and HDTMP in a 1:1 ratio offers excellent corrosion protection for carbon steel.[39] According to mass loss measurements, the corrosion rate for the control sample is 7.28 mm/year, whereas that for the Zn-HDTMP-protected sample is 2.11 mm/year, a 170% reduction in corrosion rate (Figure 11).

The filming material was collected and subjected to FT-IR, XRF and EDS studies. These show that the corrosion-inhibiting film is a material containing Zn^{2+} (from externally added Zn^{2+}) and P (from added HDTMP) in an approximate 1:4 ratio. Fe was also present, apparently

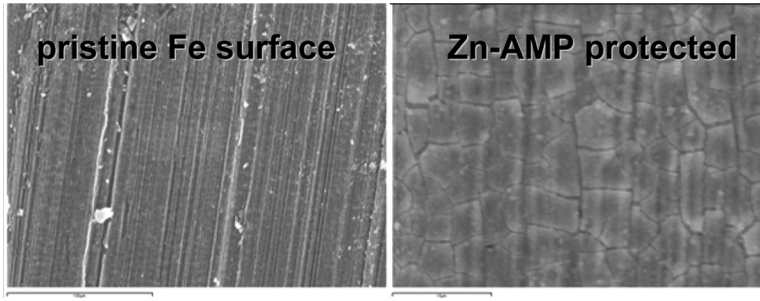

Figure 10. Zn-AMP film morphology, as shown by SEM.

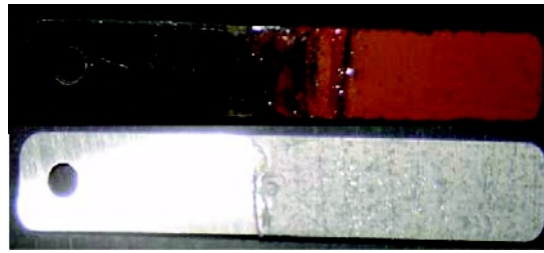

Figure 11. Corrosion protection by Zn-HDTMP (control, upper; inhibited, lower).

originating from the carbon steel specimen. FT-IR spectroscopy of the film material showed multiple bands associated with phosphonate groups that closely resemble those of the authentically prepared Zn-HDTMP material. For comparison, EDS and XRF spectra of protected and unprotected regions show the presence of Zn and P in the former, but their complete absence in the latter. Last, comparison between SEM images of the protected vs. unprotected specimen areas also demonstrate the profound anticorrosive effect of Zn-HDTMP films (Figure 12).

Additionally, the protective material acting as a corrosion barrier was studied in a similar system, but instead of Zn^{2+}, Sr^{2+}, and Ba^{2+} were used in combination with HDTMP.[51] Anticorrosion inhibitory activity

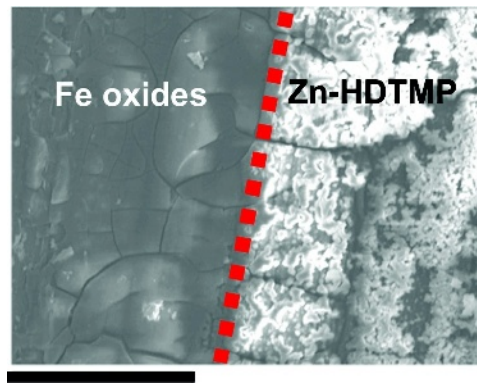

Figure 12. Zn-HDTMP film morphology. The SEM image revealed the interface (indicated by a dotted line) between the unprotected area (left) where growth of Fe oxides is evident, and the protected area (right) where a film of Zn-HDTMP had grown (bar = 100 μm).

was based on mass loss measurements. The effectiveness of corrosion protection by synergistic combinations of M^{2+} (M=Sr or Ba) and HDTMP, in a 1:1 ratio is dramatically pH-dependent. At "harsh" pH regions (2.2) mass loss from the steel specimens was profound, resulting in high corrosion rates. However, specimens 2 and 3 appeared free of corrosion products, presumably because HDTMP at the surface acted as an iron oxide dissolving agent (Figure 13). At pH 7.0 corrosion rates were appreciably suppressed in the presence of combinations of Sr^{2+} or Ba^{2+} and HDTMP (Figure 13). Corrosion rates are concentration-dependent for Sr-HDTMP, whereas they are insensitive to Ba-HDTMP levels.

The corrosion specimens at pH = 7.0 and film material were subjected to studies by VSI (see Figure 14), SEM, FT-IR, EDS, XPS studies. The inhibiting film is fairly uniform and contains M^{2+} (Sr or Ba from externally added salts) and P (from added HDTMP) in an approximate 1:2 molar ratio, suggesting a ratio of two Sr(Ba) cations and one HDTMP ligand. Comparison of the FT-IR spectra of the filming material and those for crystalline materials indicates that the molecular structure of the filming material is not the same as the structurally characterized materials.

A new metal phosphonate system was studied. Its difference from previously described systems was that a carboxyphosphonate was

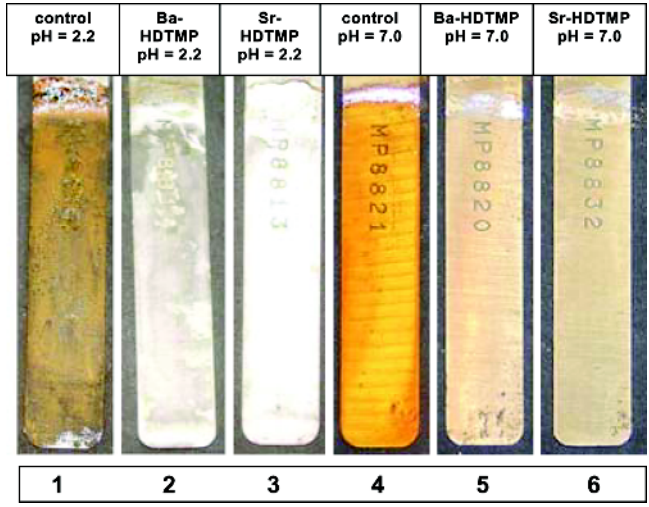

Figure 13. Anticorrosion efficiency of M-HDTMP (M=Sr or Ba) at pH 2.2 and 7.0.

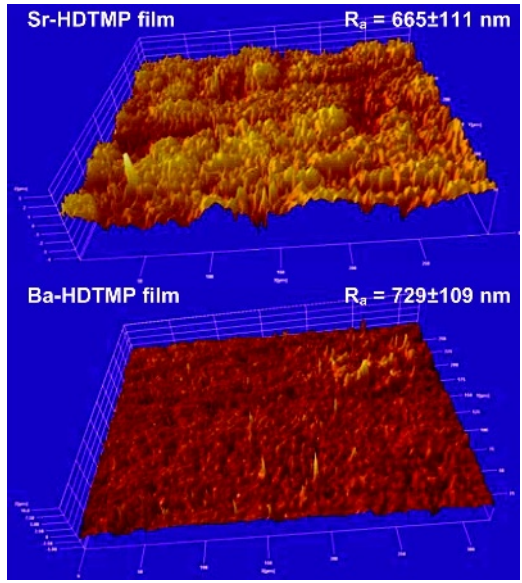

Figure 14. Anticorrosion Sr-HDTMP film morphology viewed by VSI. Grid size is $9 \times 10^4\ \mu m^2$. Z-axis is 3 μm and 10 μm for Sr-HDTMP and Ba-HDTMP films, respectively. R_a is the average surface roughness, or average deviation, of all points from a plane fit to the test part of the surface.

combined with metal ions and not a phosphonate. The goal was to ascertain whether structural changes on the organic additive backbone could offer enhancement in corrosion protection. Thus, M^{2+} ions (M=Sr, Ba) were combined with HPAA.[49,50] Anti-corrosion inhibitory activity was based on mass loss measurements. Synergistic combinations of M^{2+} and HPAA, in a 1:1 ratio and at pH = 2.0, appeared to keep the steel specimens free of corrosion products, but corrosion rates were higher than the "control" (0.299 mm/year for "control", 0.465 mm/year for Sr-HPAA and 0.397 mm/year for Ba-HPAA) (Figure 15). This was attributed to the fact that metal-HPAA combinations actually act as Fe-oxide dissolvers at pH = 2.0, rather than corrosion inhibitors. It was demonstrated that the thin layer that forms on the steel specimens and in bulk (after the corrosion experiments were left for prolonged time) was composed of Fe-HPAA. At higher pH (7.3) corrosion rates were dramatically suppressed (0.142 mm/year for the "control", 0.0005 mm/year for Sr-HPAA and 0.0005 mm/year for Ba-HPAA), reaching a virtually 100% corrosion

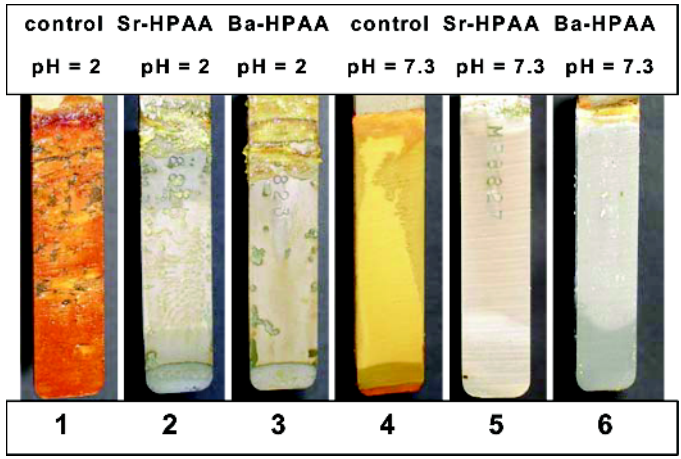

Figure 15. The anticorrosion effect of metal-HPAA films on carbon steel. Corrosion inhibition by metal-HPAA synergistic combinations is evident (specimens 2, 3, 5, and 6), compared to the "control" (specimens 1 and 4). Although specimens 2 and 3 (pH = 2.0) are free of iron oxides, corrosion rates are higher than the "control".

inhibition efficiency (Figure 15). The corrosion specimens and film material were subjected to SEM, FT-IR and EDS studies.

SEM images revealed a fairly uniform inhibiting film that contains M^{2+} (Sr or Ba from externally added salts) and P (from added HPAA), in an approximate 1:1 ratio. Fe was also present, apparently originating from the carbon steel specimen. Comparison of the FT-IR spectra of the filming material and those for crystalline materials indicates that the molecular structure of the filming material is not the same as the structurally characterized materials (*vide supra*).

Other systems were also studied. However, it was found that in these systems the metal phosphonate formed did not act as a corrosion inhibitor, but as a Fe-oxide dissolver. More specifically, a combination of Ca^{2+} and PBTC in a 1:1 molar ratio appeared to offer excellent corrosion protection for carbon steel based on visual observations (Figure 16).[46] However, based on mass loss measurements, the corrosion rate for the control sample was 0.16 mm/year, whereas for Ca-PBTC protected sample, the corrosion rate was 1.17 mm/year, which represented a 10-fold increase in the corrosion rate.

Therefore, PBTC essentially enhanced the dissolution of bare metal, presumably forming soluble Fe-PBTC complexes. The filming material

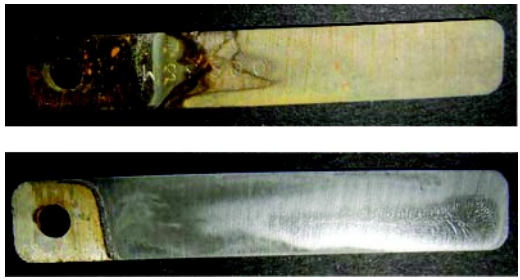

Figure 16. Phenomenology of the anticorrosive effect of Ca-PBTC films on carbon steel. The upper specimen is the "control" (upper), no inhibitor present. Surface "cleanliness" in the lower specimen (lower) by a 1 mM Ca^{2+}/PBTC equimolar combination is demonstrated, but overall metal loss is enhanced.

was collected and subjected to FT-IR, XRF and EDS studies. These show that the corrosion inhibiting film is a material containing Ca^{2+} (from externally added salt) and P (from added PBTC) in an approximate 1:1 ratio. Fe was also present apparently originating from carbon steel specimen. FT-IR of the filming material showed bands associated with the phosphonate and the carboxylate group, which closely resemble those of the authentically prepared Ca-PBTC material.

Finally, a mixture of equimolar concentrations of Ca^{2+} or Sr^{2+} and EDTMP resulted in corrosion rates that were substantially higher than the "control," 17.31 μm/y (for "control, *surface 1*) 50.60 μm/y (for Ca^{2+}, *surface 2*) and 60.38 μm/y (for Sr^{2+}, *surface 3*) (Figure 17).[52] Visual examination of specimens 2 and 3 (Figure 17) revealed that enhanced corrosion was accompanied by surface cleaning by Fe-oxide dissolution. When EDTMP (no metals, at pH 3) was used, the corrosion rate was 59.89 μm/y and the morphology of the steel surface resembled specimens 2 or 3. When the same experiments were repeated at pH 7, corrosion rate for the control was 7.62 μm/y (*surface 4*), whereas it was 27.67 μm/y for Ca^{2+} (*surface 5*) and 30.85 μm/y for Sr^{2+} (*surface 6*). As mentioned above, increased corrosion rates indicate that metal loss occurs; however, examination of the steel specimens demonstrated a dramatic chemical cleaning effect. Figure 17 shows that specimens 5 and 6 are free of corrosion products at pH 7. A similar Fe-oxide removal action was observed when PBTC (2-phosphonobutane-1,2,4-tricarboxylic acid) was used in combination with Ca^{2+} or Zn^{2+} ions (see above). Undoubtedly,

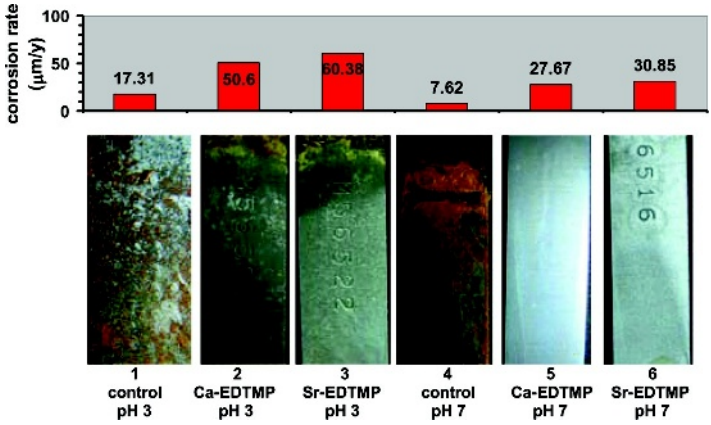

Figure 17. Micromorphology of steel specimens kept at pH 3 and pH 7. The effectiveness of Ca-EDTMP and Sr-EDTMP as Fe-oxide removers is profound at pH 3 and 7. Corrosion rates higher than the control indicate metal dissolution. Corrosion rate is calculated from the equation $CR = [534.57 \times (\text{mass loss})]/[(\text{area})(\text{time})(\text{metal density})]$. Units: CR in mm/year, mass loss in mg, area in cm^2, time in hours, metal density $= 7.85\ g/cm^3$.

high Fe-oxide removal performance was due to the presence of phosphonate moieties with high affinity for Fe^{3+}.[59]

5. DISCUSSION AND PERSPECTIVES

An ideal phosphonate corrosion inhibitor of the "complexing type" should possess the following significant attributes:

a. It must be capable of generating metal phosphonate thin films on the surface to be protected, but must not form metal phosphonate precipitates in the bulk. If the latter occurs, then corrosion protection is inefficient.
b. It should not form very soluble metal complexes, because these will not eventually "deposit" onto the metal surface, but instead will remain soluble in the bulk.
c. It should not form sparingly soluble metal complexes, because these may never reach the metal surface to achieve inhibition, but may generate undesirable deposits in the bulk or on other critical system surfaces.
d. Its metal complexes that are generated by controlled deposition on the metal surface must create dense thin films with robust structure,

thus preventing oxygen diffusion through the film and towards the metal surface. If the anticorrosion film is non-uniform or porous, then uneven oxygen permeation may create sites for localized attack, leading to uncontrollable pitting corrosion of the metal surface.

The present review has been focused on the action of metal phosphonate frameworks as potential corrosion inhibitors for water-related applications. Its epicenter was principally on the structural features of these materials. There are several hypotheses found in the literature on the mechanism of corrosion inhibition by metal-inhibitor complexes and are supported by a variety of spectroscopic and electrochemical techniques. However, none of these has unequivocally proven the molecular identity of metal-inhibitor complex.

Corrosion and its inhibition is highly pH dependent. This has been demonstrated in several systems. The general trend is that there is an enhancement of corrosion as the pH is lowered. In addition, it appears much more challenging to inhibit corrosion in the lower pH region. For example, such behavior was noted in corrosion experiments with M^{2+} (M=Sr, Ba) and HPAA (at pH = 2) or HDTMP (at pH = 2.2). Explanations for the absence of anticorrosion performance at low pH regions could be that the HPAA or HDTMP added first reacts preferentially with the Fe-oxide layer (formed almost instantaneously upon exposure of the carbon steel surface to oxygenated water) before it interacts with soluble Sr^{2+} or Ba^{2+}. Data show that at low pH regions the only material identified on the steel specimens was an amorphous (by XRD) Fe-HPAA or Fe-HDTMP compound. Both Sr^{2+} and Ba^{2+} were absent. On the other hand, results published on the action of combinations of metal ions (Ca^{2+} or Zn^{2+}) with HEDP (HEDP = hydroxyethylidene-1,1-diphosphonic acid) on carbon steel revealed that Ca^{2+} was displaced by Fe^{2+} in a "low stability" Ca-HEDP complex.[60] This did not occur for the Zn-HEDP case, resulting in a much more effective corrosion protection in the "Zn-HEDP system." A similar process of Sr^{2+} or Ba^{2+} displacement by Fe^{3+} could be envisioned in the Ba(Sr)-HDTMP system. This can explain the formation of Fe-HPAA precipitates (at pH = 2) or Fe-HDTMP precipitates (at pH = 2.2) but not of Sr^{2+} or Ba^{2+} complexes.

The ability of a metal phosphonate corrosion inhibitor to adhere onto the metal surface plays a vital role in corrosion efficacy. Bulk precipitation of a metal-phosphonate complex will lead to a loss of active

inhibitor to precipitation, leading to insufficient levels for thin-film formation. Surface adherence of the inhibitor films is a property that cannot be precisely predicted. However, it is a necessary condition for acceptable inhibition. In addition, the metal-phosphonate protective layer must be robust and uniform. A characteristic example of Zn-AMP film is shown in Figure 10 and is compared to a "bare" iron metal surface. Zn-HDTMP, Sr(Ba)-HPAA at pH = 7.3 and Sr(Ba)-HDTMP at pH = 7.0 form thin anticorrosive films that have a similar morphology.

As noted above, not all metal phosphonate systems can be effective corrosion inhibitors. The results with Ca-PBTC and Ca(or Sr)-EDTMP warrant further discussion. Corrosion rates for both systems in the presence of inhibitor are greater than those for the control (with no inhibitor). This, at first glance, is contrary to the results obtained with other systems, such as Zn-AMP, Zn-HDTMP, Sr(or Ba)-HDTMP and Sr(or Ba)-HPAA. This may be explained by several arguments. First, the metal-phosphonate film may not be robust but porous in its microscopic nature. This, as mentioned previously, would lead to localized attack and metal pitting. Such phenomena have not been observed upon examination of the metal specimens after the corrosion experiments. Second, the metal phosphonate is too soluble to deposit onto the metal surface; therefore, it does not form a protective and anticorrosion thin film. Although this argument is a logical assumption at this point, based on available literature data, more experiments must be conducted to confirm it experimentally. However, this argument would be consistent with literature data on Ca-PBTC complex formation constant (4.4), which is considered to be very low. Therefore, PBTC essentially enhances the dissolution of bare metal, presumably forming soluble Fe-PBTC complexes.

Structural differences alone cannot explain the various corrosion efficiencies observed with the present inhibitors in the presence of metal ions such as Ca^{2+}, Zn^{2+}, Sr^{2+}, Ba^{2+}. Other factors such as the solubility of the metal-phosphonate complex, complex formation ability (either in the bulk or on the metal surface), and protective film thickness and integrity certainly have a significant role. For example, the complex formation constant for Zn-AMP is 16.4 and that for Ca-PBTC is 4.4.[59] The observed more-effective corrosion protection of a Zn-AMP film compared to the corrosion inhibition of a Ca-PBTC film is consistent with the higher complex formation constant of the former. Similar arguments can be made for HDTMP; however, unfortunately, complex formation data are not available for this phosphonate. In accord with the above

arguments, variation in the corrosion rates in the case of Sr(or Ba)-HDTMP could be linked to different HDTMP complex formation constants for Sr^{2+} and Ba^{2+}. Such data are unavailable. Similar formation constants (7.10–7.56) have been reported for EDTMP.[61] Thus, differences observed in the corrosion rates may be due to the physical stability of the Sr(Ba)-HDTMP anticorrosion film.

The observed similarity in corrosion protection of a Sr-HPAA film compared to the corrosion inhibition of a Ba-HPAA film is consistent with the similar HPAA complex formation constants for Sr^{2+} and Ba^{2+}. Such data are unavailable. Similar formation constants have been reported for phosphonoformic acid.[62]

REFERENCES

1. Droffelaar, H. and J. T. N. Atkinson. 1995. *Corrosion and its Control*. Houston, NACE International.
2. Sastri, V. S. 1998. *Corrosion Inhibitors: Principles and Applications*. Chichester, Wiley, p. 720.
3. Editorial 2002. *Chem. Process.* (December), 11.B.
4. Davidson, P. *USA Today*, July 9, 2006.
5. Javaherdashti, R. 2000. *Anti-Corr. Meth. Mater.*, **47**(1): 30–34.
6. Kuznetsov, Yu. I. 1991. *Prot. Met.*, **26**: 736–744.
7. Popov, K., H. Rönkkömäki, and L. H. J. Lajunen, 2001. *Pure Appl. Chem.*, **73**: 1641–1677.
8. Sekine, I., T. Shimode, M. Yuasa, and K. Takaoka, 1992. *Ind. Eng. Chem. Res.*, **31**: 434–439.
9. Kuznetsov, Yu. I., G. Yu. Kazanskaya, and N. V. Tsirulnikova, 2003. *Prot. Met.*, **39**: 120–123.
10. Rajendran, S., B. V. Apparao, V. Periasamy, G. Karthikeyan, and N. Palaniswamy, 1998. *Anti-Corr. Meth. Mater.*, **45**(2): 109–112.
11. Felhősi, I. and E. Kálmán, 2005. *Corr. Sci.*, **47**: 695–708.
12. To, X. H., N. Pebere, N. Pelaprat, B. Boutevin, and Y. Hervaud, 1997. *Corr. Sci.*, **39**: 1925–1934.
13. Balaban-Irmenin, Yu. V., A. M. Rubashov, and N. G. Fokina, 2006. *Prot. Met.*, **42**: 133–136.
14. Fang, J. L., Y. Li, X. R. Ye, Z. W. Wang, and Q. Liu, 1993. *Corrosion*, **49**: 266–271.
15. Du, T., J. Chen, and D. Cao, 2001. *J. Mater. Sci.*, **36**: 3903–3907.
16. Frateur, I., A. Carnot, S. Zanna, and P. Marcus, 2006. *Appl. Surf. Sci.*, **252**: 2757–2769.

17. Amar, H., J. Benzakour, A. Derja, D. Villemin, and B. Moreau, 2003. *J. Electroanal. Chem.*, **558**: 131–139.
18. Paszternák, A., I. Felhősi, Zs. Keresztes, and E. Kálmán, 2007. *Mater. Sci. Forum*, **537–538**: 239–246.
19. Kuznetsov, Yu. I., G. V. Zinchenko, L. P. Kazanskii, N. P. Andreeva, and Yu. B. Makarychev, 2007. *Prot. Met.*, **43**: 648–655.
20. Amara, H., T. Braisaz, D. Villemin, and B. Moreau, 2008. *Mater. Chem. Phys.*, **110**: 1–6.
21. Ramesh, S., S. Rajeswari, and S. Maruthamuthu, 2004. *Appl. Surf. Sci.*, **229**: 214–225.
22. Dufek, E. J. and D. A. Buttry. 2008. *Electrochem. Solid-State Lett.*, **11**: C9–C12.
23. Pilbath, A., Sajo, I. Bertoti, L. Nyikos, and E. Kálmán, 2008. *Appl. Surf. Sci.*, **255**: 1841–1849.
24. Pilbáth, A., L. Nyikos, I. Bertóti, and E. Kálmán, 2008. *Corr. Sci.*, **50**: 3314–3321.
25. Shao, H. B., J. M. Wang, Z. Zhang, J. Q. Zhang, and C. N. Cao. 2002. *Mater. Chem. Phys.*, **77**: 305–309.
26. Wang, S. H., C. S. Liu, F. J. Shan, and G. C. Qi, 2008. *Acta Metall. Sin. (Engl. Lett.)*, **21**: 355–361.
27. Chougrani, K., B. Boutevin, G. David, S. Seabrook, and C. Loubat, 2008. *J. Polymer Sci. A: Polymer Chem.*, **46**: 7972–7984.
28. Deya, M., A. R. Di Sarli, B. del Amo, and R. Romagnoli, 2008. *Ind. Eng. Chem. Res.*, **47**: 7038–7047.
29. Popa, A., C.-M. Davidescu, P. Negrea, G. Ilia, A. Katsaros, and K. D. Demadis, 2008. *Ind. Eng. Chem. Res.*, **47**: 2010–2017.
30. Demadis, K. D. 2007. In *Solid State Chemistry Research Trends*, R. W., Buckley, (ed.), New York, Nova Science Publishers, pp. 109–172.
31. Murugavel, R., A. Choudhury, M. G. Walawalkar, R. Pothiraja, and C. N. R. Rao, 2008. *Chem. Rev.*, **108**: 3549–3655.
32. Clearfield, A. 2008. *Dalton Trans.*, **44**: 6089–6102.
33. Maeda, K. 2004. *Microporous Mesoporous Mater.*, **73**: 47–55.
34. Paz, F. A. A., J. Rocha, J. Klinowski, T. Trindade, F.-N. Shi, and L. Mafra, 2005. *Prog. Solid State Chem.*, **33**: 113–125.
35. Cunha-Silva, L., D. Ananias, L. D. Carlos, F. A. A. Paz, and J. Rocha, 2009. *Z. Kristallogr.*, **224**: 261–272.
36. Demadis, K. D., S. D. Katarachia, and M. Koutmos. 2005. *Inorg. Chem. Commun.*, **8**: 254–258.
37. Daly, J. J. and P. J. J. Wheatley. 1967. *Chem. Soc. A*, 212–221.
38. Mao, J.-G., Z. Wang, and A. Clearfield, 2002. *New J. Chem.*, **26**: 1010–1014.
39. Demadis, K. D., C. Mantzaridis, R. G. Raptis, and G. Mezei, 2005. *Inorg. Chem.*, **44**: 4469–4471.

40. Liang, J. and G. K. H. Shimizu, 2007. *Inorg. Chem.*, **46**: 10449–10451.
41. Hix, G. B., B. M. Kariuki, S. Kitchin, and M. Tremayne. 2001. *Inorg. Chem.*, **40**: 1477–1481.
42. Ortiz-Avila, Y., P. R. Rudolf, and A. Clearfield, 1989. *Inorg. Chem.*, **28**: 2137–2141.
43. Song, J.-L. and J.-G. Mao. 2005. *J. Mol. Struct.*, **740**: 181–186.
44. Gómez-Alcantara, M. M., M. A. G. Aranda, P. Olivera-Pastor, P. Beran, J. L. García-Muñoz, and A. Cabeza. 2006. *Dalton Trans.*, 577–585.
45. Gómez-Alcantara, M. M., A. Cabeza, M. A. G. Aranda, A. Guagliardi, J. G. Mao, and A. Clearfield. 2004. *Solid State Sci.*, **6**: 479–487.
46. Demadis, K. D., P. Lykoudis, R. G. Raptis, and G. Mezei. 2006. *Cryst. Growth Des.*, **6**: 1064–1067.
47. Demadis, K. D., J. D. Sallis, R. G. Raptis, and P. Baran, 2001. *J. Am. Chem. Soc.*, **123**: 10129–10130.
48. Kato, Y., L. M. Toledo, J. Rebek, Jr. 1996. *J. Am. Chem. Soc.*, **118**: 8575–8579.
49. K. D. Demadis, M. Papadaki, R. G. Raptis, and H. Zhao, 2008. *J. Solid State Chem.*, **181**: 679–683.
50. Demadis, K. D., M. Papadaki, R. G. Raptis, and H. Zhao, 2008. *Chem. Mater.*, **20**: 4835–4846.
51. Demadis, K. D., E. Barouda, R. G. Raptis, and H. Zhao, 2009. *Inorg. Chem.*, **48**: 819–821.
52. Demadis, K. D., E. Barouda, N. Stavgianoudaki, and H. Zhao. 2009. *Cryst. Growth Des.*, **9**: 1250–1253.
53. Mondry, A. and R. Janicki. 2006. *Dalton Trans.*, 4702–4710.
54. Janicki, R. and A. Mondry, 2008. *Polyhedron*, **27**: 1942–1946.
55. Kálmán, E., I. Lukovits, and G. Palinkas, 1995. *ACH-Models Chem.*, **132**: 527–533.
56. Bofardi, B. P. 1993. In *Reviews on Corrosion Inhibition Science and Technology*, Raman, A. and Labine, P., (eds.), Houston, TX, NACE International, pp. 2–6.
57. Gunasekaran, G., N. Palanisamy, B. V. Appa Rao, and V. S. Muralidharan, 1997. *Electrochim. Acta.*, **42**: 1427–1434.
58. NACE Standard TM0169–95 (item no. 21200).
59. Knepper, T. P. 2003. *Trends Anal. Chem.*, **22**: 708–724.
60. Awad, H. S. and S. Turgoose, 2004. *Corrosion*, **60**: 1168–1179.
61. Sawada, K., T. Miyagawa, T. Sakaguchi, and K. Doi. 1993. *Dalton Trans.*, 3777–3784.
62. Song, B., D. Chen, M. Bastian, R. B. Martin, and H. Sigel, 1994. *Helv. Chim. Acta.*, **77**: 1738–1756.